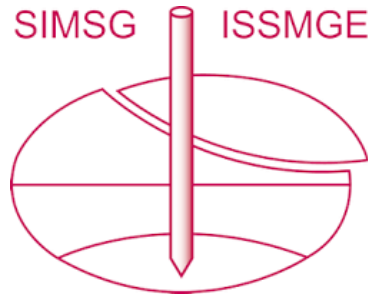


INTERNATIONAL SOCIETY FOR SOIL MECHANICS AND GEOTECHNICAL ENGINEERING



This paper was downloaded from the Online Library of the International Society for Soil Mechanics and Geotechnical Engineering (ISSMGE). The library is available here:

<https://www.issmge.org/publications/online-library>

This is an open-access database that archives thousands of papers published under the Auspices of the ISSMGE and maintained by the Innovation and Development Committee of ISSMGE.

The paper was published in the proceedings of the 10th European Conference on Numerical Methods in Geotechnical Engineering and was edited by Lidija Zdravkovic, Stavroula Kontoe, Aikaterini Tsiampousi and David Taborda. The conference was held from June 26th to June 28th 2023 at the Imperial College London, United Kingdom.

To see the complete list of papers in the proceedings visit the link below:

<https://issmge.org/files/NUMGE2023-Preface.pdf>

Assessment of the state parameter used in two-surface plasticity models

A. Dilip¹, O. Adamidis¹

¹*Department of Civil Engineering, University of Oxford, Oxford, UK*

ABSTRACT: Two-surface plasticity models are very popular for modelling liquefaction-related problems. Central to their formulation is the state parameter, a measure of how far the current soil state is from the critical state. The bounding and dilatancy surfaces are typically defined as functions of the state parameter, which allows them to evolve and eventually collapse on the critical surface, at critical state. In this paper, we revisit the definition of the state parameter within the framework of two-surface plasticity models, using partially drained triaxial compression tests on Hostun sand, under a constant ratio of volumetric to axial strain. We first demonstrate analytically and numerically how post phase transformation instability points in coupled strain triaxial compression tests can be used to isolate the state parameter. We then perform partially drained triaxial tests to experimentally derive a constant state parameter curve, which we use to assess the current state parameter definition. We expect the results to be of particular interest for modelling the partially drained response of sands.

Keywords: Two-surface plasticity models; constitutive modelling; element testing; state parameter; partial drainage; Hostun sand.

1 INTRODUCTION

Numerical modelling for liquefaction-related problems is a methodology that has gained much momentum in the last decade. Advanced constitutive models that capture the complex behaviour of sand under undrained cyclic loading, are typically used in such numerical simulations (e.g., Boulanger and Ziotopoulou, 2015; Prevost, 1985; Taiebat and Dafalias, 2008). Robust constitutive models are essential to reliably simulate the complex material behaviour observed in liquefaction-related phenomena. The SANISAND family of two-surface plasticity models is the preferred choice for many researchers due to the capability of such models to replicate both monotonic and cyclic behaviour with a unique set of model constants across all densities and confining pressures. A simple outline of two-surface plasticity models is given by Dafalias and Manzari (2004).

The SANISAND formulations incorporate the state parameter as a way to relate peak stress-ratio and dilatancy to critical-state soil mechanics (CSSM). The state parameter provides an indication of the relative ‘distance’ of the current soil state from the critical state (Been and Jeffries, 1985). It is defined as the vertical distance between the current state and the critical state (CS) in a void ratio (e)-mean effective stress (p') plot. This study aims to investigate the reliability of this definition within SANISAND models, with regards to representing soil behaviour under partially drained conditions. Partial drainage has been shown to be important for a range of liquefaction-related phenomena, from the triggering of liquefaction (Cubrinovski et al., 2019) and

the co-seismic evolution of pore pressures and displacements (Adamidis and Madabhushi, 2018), to post-earthquake slope stability (Malvick et al., 2008).

Despite the importance of partial drainage, constitutive models for liquefaction are rarely assessed for their performance under such conditions. Here, the version of SANISAND presented by Taiebat and Dafalias (2008) is implemented to model sand behaviour in triaxial stress space. A constant state parameter curve is identified analytically and obtained numerically using the locus of instability points occurring post phase transformation in triaxial compression tests, under a constant ratio of volumetric to axial strain. A constant state parameter curve is then produced experimentally from similar, coupled strain triaxial compression tests on Hostun sand. The numerical and experimental constant state parameter curves are compared and an updated definition for the state parameter is proposed.

2 CONSTITUTIVE MODELLING

The SANISAND 2008 model (Taiebat and Dafalias, 2008) has a narrow conical wedge-type yield surface in triaxial stress space with the wedge bisector or back-stress ratio denoted by α and a closed cap in the mean effective stress direction (Figure 1). The rotational hardening, $\hat{\alpha}$ simulates the evolution of anisotropy under a varying stress ratio, $\eta (= \frac{q}{p'})$. The isotropic hardening rule governed by the end cap captures the accumulation of plastic strains at high confining pressures under a

constant stress ratio. The plastic volumetric and shear strains are represented in two parts: the first part induced by a varying stress-ratio and the second part induced by a constant stress-ratio.

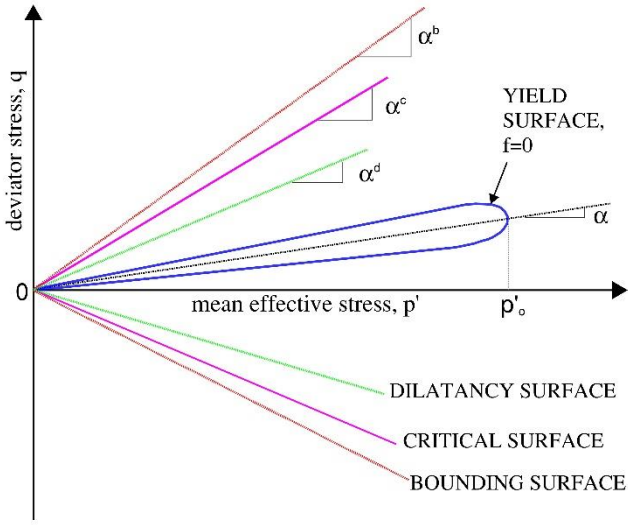


Figure 1. Schematic illustration of model surfaces in triaxial space

The bounding surface (α^b) and the dilatancy surface (α^d) evolve based on the critical surface (α^c) and the state parameter (ψ) in a CSSM framework, as shown in Equations (1-2), where n^b and n^d are model parameters.

$$\alpha^b = \alpha^c \cdot e^{(-n^b \cdot \psi)} \quad (1)$$

$$\alpha^d = \alpha^c \cdot e^{(n^d \cdot \psi)} \quad (2)$$

Using the constitutive formulations in triaxial space, the elastic stiffness matrix (D_e) and the elastoplastic stiffness matrix (D_{ep}) for monotonic compression tests and for $p' \ll p'_o$, are computed and shown in Equations (3-4).

$$D_e = \begin{bmatrix} K & 0 \\ 0 & 3G \end{bmatrix} \quad (3)$$

$$D_{ep} = \begin{bmatrix} \frac{p'HK+3GKs}{p'H+3Gs-DK\eta} & \frac{-3GKD}{p'H+3Gs-DK\eta} \\ \frac{3GK\eta s}{p'H+3Gs-DK\eta} & \frac{3Gp'H-3GKD\eta}{p'H+3Gs-DK\eta} \end{bmatrix} \quad (4)$$

with K the elastic bulk modulus; G the elastic shear modulus; H the hardening modulus [= $h(\alpha^b - \alpha)$, where h is a positive hardening parameter]; and D the dilatancy [= $sA_d(\alpha^d - \alpha)$, where A_d is a dilatancy parameter and s is a model parameter, taken as +1 for compression tests].

The model was implemented in triaxial space in MATLAB, using the forward Euler method and strain-controlled loading steps. The model parameters used for

Toyoura sand are shown in Table 1 and are those suggested by Taiebat and Dafalias (2008). Default values were used for the following parameters: $m = 0.05\alpha^c$, $n = 20$, $V = 1000$ and $P_{at} = 98.06 \text{ kPa}$.

Table 1. SANISAND model parameters for Toyoura sand

Parameter	Symbol	Value
Elasticity	G_0 (kPa)	125
	K_0 (kPa)	150
CSL	α_c^c	1.2
	e_0	0.934
	λ	0.019
Dilatancy	ξ	0.7
	n^d	2.1
	A_d	0.4
Kinematic Hardening	n^b	1.25
	h_0	36.96
	c_h	0.987

2.1 Undrained monotonic test results

The purpose of this initial calibration was to verify that the current implementation performs as expected when compared to published results. Undrained monotonic tests were simulated for a range of void ratios and initial effective confining pressures ($p' \ll p'_o$), following the experimental and numerical data presented by Taiebat and Dafalias (2008). Simulations for dense Toyoura sand are presented in Figure 2 and show good agreement with published results.

2.2 Partially drained monotonic test results

Coupled strain paths were imposed numerically, using the calibration described above. The coupled strain paths corresponded to constant ratios of volumetric strain rate ($\dot{\epsilon}_v$) to axial strain rate ($\dot{\epsilon}_1$). A positive rate indicates water flow out of the specimen and a negative rate indicates water flow into the specimen. Indicative results are shown in Figure 3, for varying coupling ratios, including the undrained condition.

Coupled strain paths were previously simulated for Direct Simple Shear (DSS) tests by Kamai and Boulanger (2012), using the PM4SAND constitutive model (Boulanger and Ziotopoulou, 2015), based on a two-surface plasticity framework similar to SANISAND. The current simulation results qualitatively agree with the results obtained in the DSS simulations, as well as with the experimental triaxial tests conducted by Vaid and Eliadorani (1998).

As seen from Figure 3, at 100 kPa initial confining pressure, the soil behaves in a dilative manner under undrained conditions. For water outflow conditions, strain hardening is observed. Under an inflow condition, an initially strain-hardening response turns to strain-softening at larger strains; a peak in deviator stress is observed as a result. Under undrained conditions, a peak in deviator stress is also an instability point. Under a

water inflow condition, instability points have to be determined using Hill's stability criterion. This process,

outlined below, is essential in identifying constant state parameter lines.

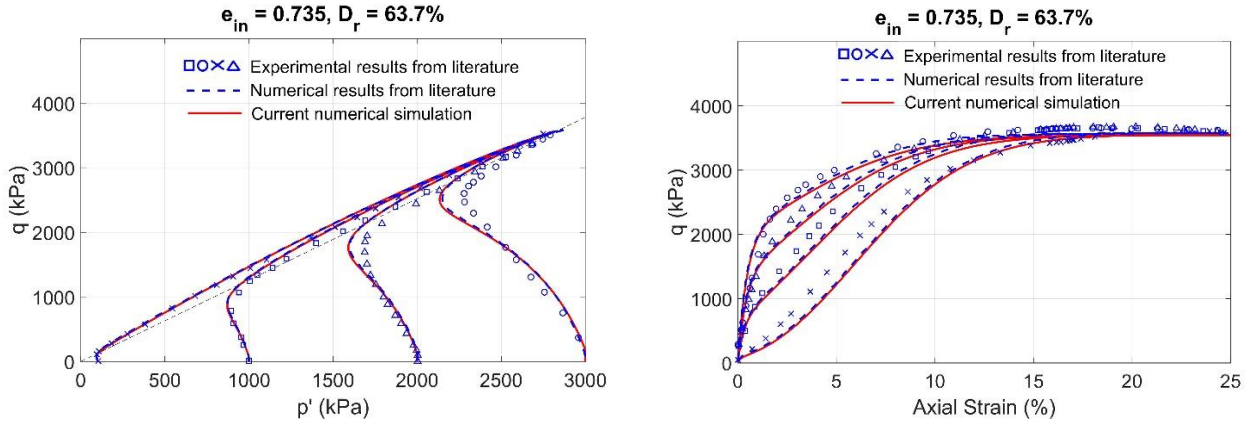


Figure 2. Comparison of experimental data and simulations for undrained triaxial compression tests on isotropically consolidated samples of Toyoura sand (initial void ratio, $e_{in} = 0.735$; relative density, $D_r = 63.7\%$)

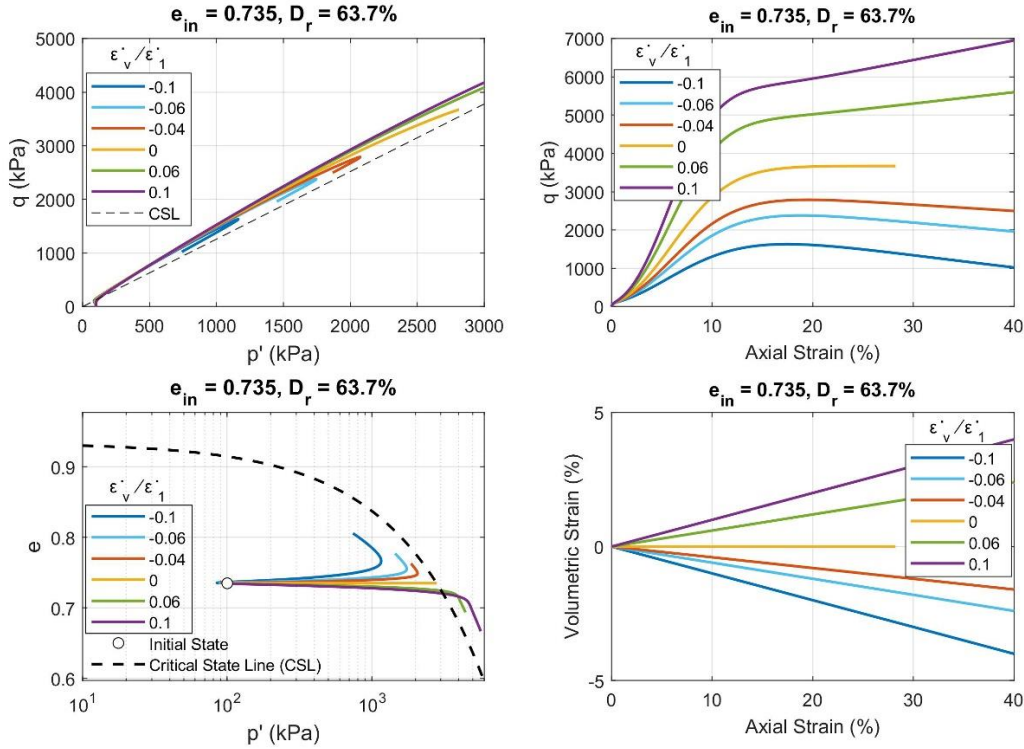


Figure 3. Simulations for partially drained triaxial tests on isotropically consolidated samples of Toyoura sand for varying strain ratios $\dot{\epsilon}_v/\dot{\epsilon}_1$ (relative density, $D_r = 63.7\%$ and initial mean effective stress, $p'_{in} = 100$ kPa)

3 INSTABILITY POINTS UNDER COUPLED STRAIN PATH

Andrade et al. (2013) numerically simulated undrained compression behaviour and imposed a loss of uniqueness condition to detect instability. They related the instability to a limiting hardening modulus that is dependent on soil state. A similar approach is undertaken to predict instability under coupled strain paths.

3.1 Hill's stability criterion

The loss of uniqueness condition stems from Hill's stability criterion, often used to determine instability in a

material. Hill postulated that if the second-order of work (\dot{W}) is strictly positive, the material is stable. Andrade et al. (2013) expressed Hill's stability criterion for triaxial tests in terms of effective stress increments (\dot{p}' and \dot{q}) and strain increments ($\dot{\epsilon}_v$ and $\dot{\epsilon}_q$), as in Equation (5).

$$\dot{W} = \dot{p}' \cdot \dot{\epsilon}_v + \dot{q} \cdot \dot{\epsilon}_q > 0 \text{ for stability} \quad (5)$$

3.2 Limiting hardening modulus

The second-order of work shown in Equation (5) was obtained for the compression tests simulated here, using

the imposed strain increments for a selected strain coupling ratio ($\Gamma = \dot{\epsilon}_v/\dot{\epsilon}_1$) and the elastoplastic constitutive relations of Equations (3-4). Instability was detected when the second-order of work changed from positive to negative. Detected instability points are shown in Figure 4 with star markers.

A limiting hardening modulus (H_L) that determines the onset of instability is shown in Equations (6-7). It is calculated for a given strain coupling ratio ($\Gamma = \dot{\epsilon}_v/\dot{\epsilon}_1$)

and under undrained conditions ($\Gamma = 0$), it matches that of Andrade et al. (2013).

$$H_L = \frac{3GK(D-s\Lambda)(\eta+\Lambda)}{p'(\kappa\Lambda^2+3G)} \quad (6)$$

$$\Lambda = \frac{\dot{\epsilon}_v}{\dot{\epsilon}_q} = \frac{3\Gamma}{3-\Gamma} \quad (7)$$

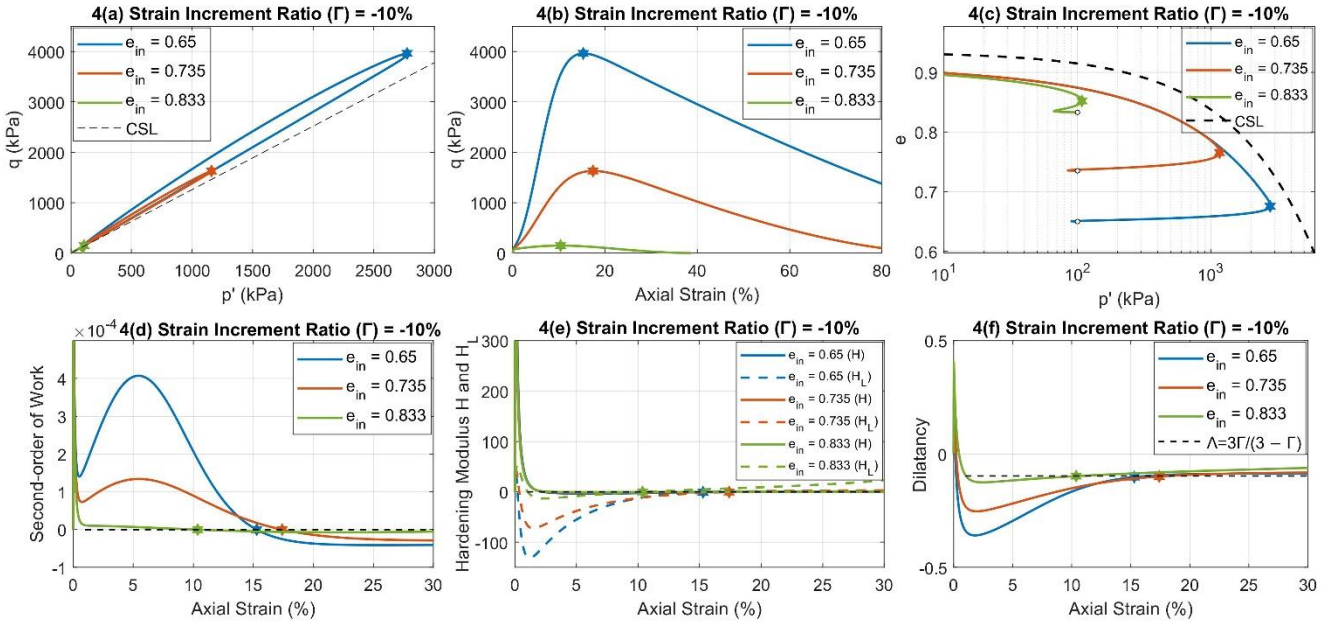


Figure 4. Simulations for partially drained triaxial tests on isotropically consolidated samples of Toyoura sand for $\Gamma = -10\%$ (initial mean effective stress, $p'_{in} = 100$ kPa)

3.3 Instability line

The results shown in Figure 4(e) indicate that at the identified instability points, the limiting hardening modulus, $H_L \rightarrow 0$. From Equation (6), it can be deduced that either the dilatancy parameter, $D \rightarrow s\Lambda$ (with $s = +1$ for monotonic compression) or $\eta \rightarrow -\Lambda$. From Figure 4(a) $p' - q$ plot, it can be easily observed that $\eta \neq -\Lambda$. Hence, $D \rightarrow s\Lambda$. This is confirmed in Figure 4(f), where the constant value of Λ is superposed on the plot of dilatancy D .

Using Equations (1-2, 6-7) and taking $s = +1$ for monotonic compression, an expression can be produced for the identified instability points:

$$\begin{aligned} H &= h(\alpha^b - \alpha) = H_L = 0 \\ \Rightarrow \alpha^b &= \alpha \end{aligned} \quad (8)$$

$$\begin{aligned} \text{From Equation (6), } D - s\Lambda &= 0 : \\ \Rightarrow sA_d(\alpha^d - \alpha) &= s\Lambda \\ \Rightarrow A_d(\alpha^d - \alpha^b) &= \Lambda \\ \Rightarrow A_d \cdot \alpha^c (e^{n^d \cdot \psi} - e^{-n^b \cdot \psi}) &= \Lambda \end{aligned} \quad (9)$$

From Equation (7), Equation (9):

$$A_d \cdot \alpha^c (e^{n^d \cdot \psi} - e^{-n^b \cdot \psi}) = \frac{3\Gamma}{3-\Gamma} \quad (10)$$

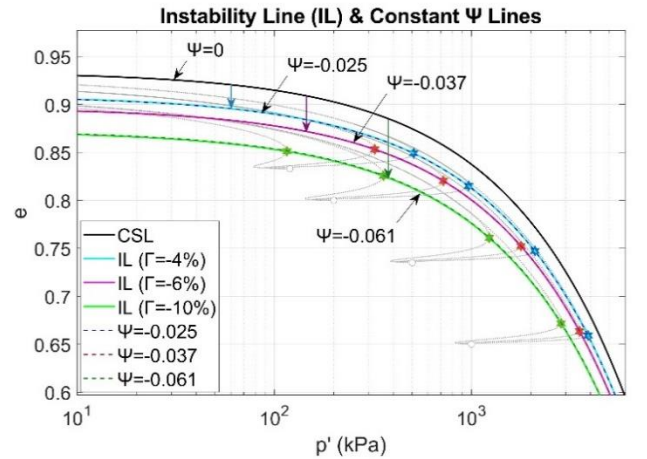


Figure 5. Instability lines or constant Ψ lines for coupled strain paths under $\Gamma = -4\%$, -6% and -10%

Equation (10) represents the locus of instability points for a given strain coupling ratio Γ . It shows that for a given strain coupling ratio Γ , instability points will lie on a curve of a corresponding state parameter, ψ . Equation (10) is plotted in the $e - p'$ space in Figure 5

for three strain coupling ratios Γ . A plethora of stress paths under the same coupling strain ratios are also plotted, with the instability points derived from Equation (5) added in star markers. Equation (10) is shown to accurately represent the locus of instability points across a range of initial conditions and Γ values.

This theoretical exercise demonstrates that for two-surface plasticity models of the SANISAND family, Equation (10) represents an ‘instability curve’ for a given strain coupling ratio Γ and corresponds to a constant state parameter ψ . An experimental campaign follows, whose aim was to identify such instability points for a given Γ so as to experimentally derive an ‘instability curve’ as in Equation (10) and thus assess what a constant state parameter curve should look like.

4 EXPERIMENTAL TESTING

Initially drained and undrained monotonic triaxial tests were undertaken to locate the critical state line (CSL). Additionally, partially drained triaxial tests under a constant strain coupling ratio Γ were performed.

4.1 Testing equipment

The experiments were performed using a GDS advanced dynamic triaxial testing system at the University of Oxford. The tests presented here were conducted under strain-controlled monotonic compression. The back-pressure controller was used to control volume flow into and out of the specimen.

4.2 Testing material and testing protocol

All tests were performed on Hostun HN31 sand. Detailed sand properties can be found in Adamidis and Anastasopoulos (2022). Specimens were cylindrical, 70mm in diameter and 140mm in height. Water (wet) pluviation was used for sample preparation. The testing protocol was based on ASTM D4767-11 for undrained tests and ASTM D7181-11 for drained tests. The B-values for all tests were between 95% to 98%.

The specimens were isotropically consolidated to the required mean effective stress at a rate of 33 kPa/hr. The shearing stage was commenced the next day with imposed axial displacement rates of 6mm/hr for undrained tests and 3mm/hr for drained tests. The partially drained triaxial tests were conducted by imposing an axial displacement rate of 6mm/hr and an inflow volumetric strain rate of 10% of the axial strain rate. Membrane correction and barrelling were considered, assuming a parabolic deformed shape. Membrane penetration effects were negligible.

4.3 Critical state line determination

The conducted monotonic compression tests are shown in Figure 6 with red lines. The proposed expression for

the CSL (Equation 11) is shown in purple in Figure 6 and was also based on tests conducted by the second author (OA) in ETH Zurich (see Adamidis and Anastasopoulos, 2022 for information on experimental methods) and on published results by Azeiteiro et al. (2017) and Konrad (1993).

$$e_{cs} = e_{max} - \frac{(e_{max} - e_{min})R}{Q - \ln(p')} \quad (11)$$

with e_{cs} the void ratio at critical state; e_{max} the maximum void ratio ($= 1.049$); e_{min} the minimum void ratio ($= 0.671$); $R = 1.2$ and $Q = 8.8$.

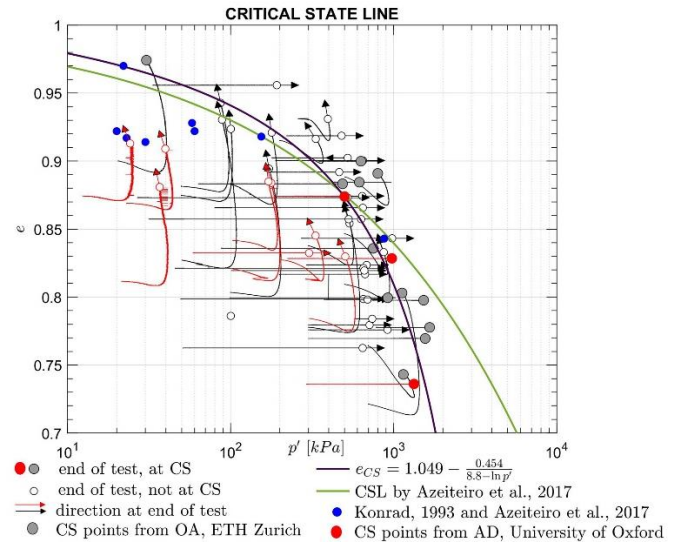


Figure 6. Critical state line for Hostun sand

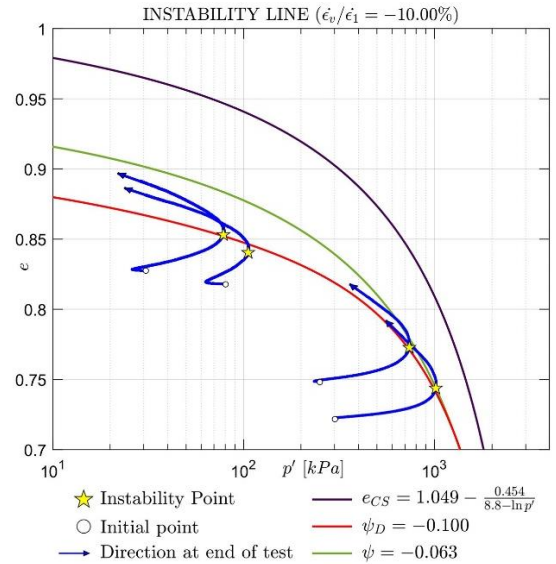


Figure 7. Partially drained monotonic triaxial tests under $\varepsilon_v/\varepsilon_1 = -10\%$ and corresponding instability line

4.4 Partially drained test results

The results of the monotonic triaxial compression tests performed under a constant ratio of volumetric strain rate to axial strain rate, $\varepsilon_v/\varepsilon_1 = -10\%$ are plotted in $e -$

p' space in Figure 7. The instability points were calculated using Equation (5).

4.5 Instability curve

The current definition of the state parameter ψ , shown with a green line in Figure 7, does not match well the locus of the experimentally derived instability points. An updated state parameter ψ_D is proposed instead for Hostun sand, described in Equation (12).

$$\psi_D = (e - e_{cs}) \frac{(a+pp')}{(a+bp')} \quad (12)$$

where e_{cs} is the void ratio at critical state; $a = 800$ and $b = 0.4$.

For a constant updated state parameter ψ_D , the vertical distance from the CSL in $e - p'$ space is reduced as p' increases. For the coupled strain ratio, $\varepsilon_v/\varepsilon_1 = -10\%$ the value for the constant updated state parameter that matches the locus of instability points is $\psi_D = -0.1$. This exercise has indicated that the current definition of the state parameter within two-surface plasticity models might need to be updated, especially when it comes to capturing the behaviour of soils under partially drained conditions.

5 CONCLUSION

This paper represents an effort to isolate and assess the state parameter used in two-surface plasticity models. The method is inspired by loading under partially drained, or rather, non-undrained conditions. Drainage, especially when resulting in volumetric expansion, can lead to liquefaction triggering even for soils that are stable under undrained loading. This can greatly impact the behaviour of sands, for instance due to upwards dissipating pore water during and after an earthquake.

Monotonic triaxial compression paths, where the volumetric strain rate is coupled to the axial strain rate were numerically modelled using the SANISAND 2008 constitutive model. Post phase transformation instability points were then located using Hill's stability criterion. It was shown that the locus of all such points for a given rate of strain coupling lie on a constant state parameter line. Monotonic triaxial compression tests with coupled volumetric and axial strains were then experimentally conducted on Hostun sand, to obtain what according to the used constitutive model should be a constant state parameter line. The experimental results suggested that an update in the definition of the state parameter is required to replicate the observed behaviour. The updated definition of the state parameter is expected to improve the performance of two-surface plasticity constitutive models under conditions of partial drainage.

6 ACKNOWLEDGEMENTS

The authors would like to thank University College, University of Oxford for providing funds to pursue this research.

7 REFERENCES

- Adamidis, O., Anastasopoulos, I. 2022. Cyclic liquefaction resistance of sand under a constant inflow rate. *Géotechnique*, 1-14.
- Adamidis, O., Madabhushi, S.P.G. 2018. Experimental investigation of drainage during earthquake-induced liquefaction. *Géotechnique* **68(8)**, 655-665.
- Andrade, J.E., Ramos, A.M., Lizcano, A. 2013. Criterion for flow liquefaction instability. *Acta Geotechnica* **8(5)**, 525-535.
- Azeiteiro, R.J., Coelho, P.A., Taborda, D.M., Grazina, J.C. 2017, May. Critical state-based interpretation of the monotonic behaviour of Hostun sand. American Society of Civil Engineers.
- Been, K., Jefferies, M.G. 1985. A state parameter for sands. *Géotechnique* **35(2)**, 99-112.
- Boulanger, R.W., Ziotopoulou, K. 2015. PM4Sand (Version 3): A sand plasticity model for earthquake engineering applications. *Center for Geotechnical Modeling Report No. UCD/CGM-15/01, Department of Civil and Environmental Engineering, University of California, Davis, Calif.*
- Cubrinovski, M., Rhodes, A., Ntritsos, N., Van Ballegooy, S. 2019. System response of liquefiable deposits. *Soil Dynamics and Earthquake Engineering* **124**, 212-229.
- Dafalias, Y.F., Manzari, M.T. 2004. Simple plasticity sand model accounting for fabric change effects. *Journal of Engineering mechanics* **130(6)**, 622-634.
- Kamai, R., Boulanger, R.W. 2012. Single-element simulations of partial-drainage effects under monotonic and cyclic loading. *Soil Dynamics and Earthquake Engineering* **35**, 29-40.
- Konrad, J.M. 1993. Undrained response of loosely compacted sands during monotonic and cyclic compression tests. *Géotechnique* **43(1)**, 69-89.
- Malvick, E.J., Kutter, B.L., Boulanger, R.W. 2008. Postshaking shear strain localization in a centrifuge model of a saturated sand slope. *Journal of geotechnical and geoenvironmental engineering* **134(2)**, 164-174.
- Prevost, J.H. 1985. A simple plasticity theory for frictional cohesionless soils. *International Journal of Soil Dynamics and Earthquake Engineering* **4(1)**, 9-17.
- Taiebat, M., Dafalias, Y.F. 2008. SANISAND: Simple anisotropic sand plasticity model. *International Journal for Numerical and Analytical Methods in Geomechanics* **32(8)**, 915-948.
- Vaid, Y.P., Eliadorani, A. 1998. Instability and liquefaction of granular soils under undrained and partially drained states. *Canadian Geotechnical Journal* **35(6)**, 1053-1062.